Contribution from the Istituto di Chimica dell'Università di Trieste, 34127, Trieste, Italy

MO Studies for Transition Metal Complexes with Polydentate Ligands. II. Electronic Structure and Related Properties of $Fe^{II}(Dmg)_2L_2$ and $Co^{III}(Dmg)_2L_2$ Complexes

G. De Alti, V. Galasso, A. Bigotto and G. Costa

Received July 10, 1969

The bonding in Fe^{II}- and $Co^{III}(Dmg)_2L_2$ complexes is described in terms of molecular orbitals, particular attention being devoted to the effects of the σ-donor capabilities of nitrogen-containing axial ligands. The interpretation of the electronic spectra as given on the basis of the calculated one-electron transitions and the behaviour of the principal parameters of the ^{57}Fe Mössbauer spectra are discussed.

Introduction

Complexes of the type M(chel)XY, where M is Fe or Co, « chel » an equatorial tetradentate nitrogen-containing chelating agent and X, Y axial ligands in an essentially octahedral arrangement, are being investigated as model molecules of compounds of biological importance, like Vitamin B_{12} and haemoglobin. Many important problems of electronic effects through the metal atom (ground state, thermodynamic and kinetic *cis* and *trans* effect),[1] are implied in the elucidation of the properties of the naturally occurring and model molecules.

Though qualitative pictures of the electronic structure were previously presented, the MO investigations for this type of compounds are limited to Fe and Co porphyrins.[3]

In the previous paper[4] some general problems as the use of sophisticated atomic functions, the extension of charge-dependence to the VSIE of ligand orbitals and the parameterization of σ and π interactions were examined. Now, in order to describe the effect of the axial ligand on the in-plane system as derived from the charge donated to the metal and transmitted to the equatorial system,[5] we confine our attention to the influence of the σ-donor power of nitrogen bases as axial ligands L on the electronic structure of simple models of the type $M(Dmg)_2L_2$ where $(Dmg)_2$ is the bis-dimethylglyoximato dianion and M is Co^{III} or Fe^{II}.

The influence of the macrocycle is exerted through the 2pσ-orbitals of nitrogen and 2pπ orbitals of nitrogen, carbon and oxygen atoms, while the axial ligand participates to the bond only with the 2pσ orbital of nitrogen atom. In order to account for different σ-donor properties of the axial ligands different energy values have been assigned to the 2pσ orbital of the axial nitrogen atom.

The calculated electronic structures provide informations on the changes of metal orbital configuration, atomic charges, π-delocalization on the molecular framework and overlap populations of the relevant bonds. The one-electron transitions, even if calculated without taking into account the interelectronic repulsions, give at least qualitative elucidation of the experimental bands sensitive to the changes of donor power of axial ligands. Previsions are also afforded for the quadrupole splitting of ^{57}Fe Mössbauer spectra.

Finally, the $Co^{II}(Dmg)_2L_2$ complexes were considered in connection with the orbital assignment of the unpaired electron, as inferred from ESR spectra.

Details of Calculation. The assumed geometry of the models is that of $Co^{III}(Dmg)_2(NH_3)_2$[6] reported in Figure 1.

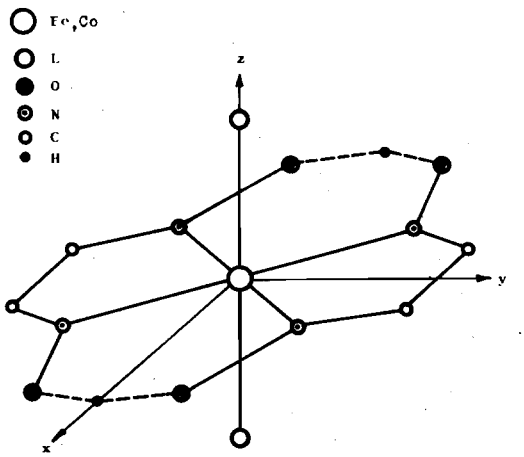

Figure 1. Structure of the complex $M(Dmg)_2L_2$

(1) See *e.g.* H. A. Hill and K. G. Morallee, *J. Chem. Soc.*, (A) *1969*, 554; G. Costa, G. Tauzher and A. Puxeddu, *Inorg. Chim. Acta*, 3, 41 (1969).
(2) B. W. Dale, R. J. P. Williams, P. R. Edwards and C. E. Johnson, *Trans. Far. Soc.*, *64*, 620 (1968).
(3) M. Zerner, M. Gouterman and H. Kobayashi, *Theoret. Chim. Acta*, 6, 363 (1966), and preceding papers; K. Ohno, Y. Tanabe and F. Sasaki, *Theorct. Chim. Acta*, *1*, 378 (1963).
(4) G. De Alti, V. Galasso and A. Bigotto, *Inorg. Chim. Acta*, 3, 527 (1969).
(5) P. Day, *Theoret. Chim. Acta*, 7, 328 (1967).
(6) K. R. Viswanathan and N. R. Kunchur, *Acta Crystall*, *14*, 675 (1961).

Table I. Electronic population of metal orbitals and net charges

Complex	Iron				Cobalt			
Case	A	B	C	D	A	B	C	D
3d	6.9658	6.9545	6.9406	6.9347	7.8136	7.7867	7.7561	7.7402
4s	0.5247	0.5223	0.5076	0.4933	0.5859	0.6060	0.6047	0.5945
4p	0.3367	0.2815	0.2718	0.2692	0.4269	0.3609	0.3510	0.3499
Metal	0.1728	0.2417	0.2800	0.3028	0.1736	0.2464	0.2882	0.3154
N	−0.0672	−0.0086	0.0248	0.0442	0.0541	0.1260	0.1720	0.2010
C	0.1399	0.1676	0.1765	0.1806	0.1695	0.1961	0.2035	0.2069
O	−0.4386	−0.4366	−0.4360	−0.4358	−0.4363	−0.4346	−0.4344	−0.4343
L[a]	0.6454	0.4343	0.3294	0.2706	0.8386	0.6018	0.4736	0.3952

[a] L stands for axial nitrogen atom.

Table II. Partial and total bond orders for bonds M—N and M—L[a]

	Complex	Iron				Cobalt			
	Case	A	B	C	D	A	B	C	D
	$3d_{x^2-y^2}$	0.0040	0.0048	0.0052	0.0058	0.0040	0.0050	0.0060	0.0066
	$3d_{z^2}$	0.0724	0.0842	0.0918	0.0976	0.0716	0.0908	0.1056	0.1148
	$3d_{xy}$	0.2830	0.3004	0.3102	0.3434	0.3293	0.3360	0.3366	0.3354
	4s	0.2820	0.2850	0.2860	0.3612	0.3436	0.3404	0.3334	0.3266
	$4p_y$	0.0958	0.1070	0.1132	0.1226	0.1114	0.1254	0.1346	0.1402
	$4p_x$	0.0798	0.0886	0.0938	0.1024	0.0924	0.1036	0.1112	0.1158
Bond M—N	σ—Total	0.8170	0.8700	0.9002	1.0330	0.9523	1.0012	1.0274	1.0394
	$3d_{yz}$	0.1180	0.1036	0.0950	0.1100	0.0694	0.0594	0.0824	0.0598
	$3d_{xz}$	0.0074	0.0052	0.0040	0.0040	0.0016	0.0002	−0.0008	0.0014
	$4p_z$	0.0674	0.0422	0.0408	0.0542	0.0838	0.0502	0.0464	0.0486
	σ—Total	0.1928	0.1510	0.1393	0.1582	0.1548	0.1098	0.1280	0.1098
	σ+π Total	1.0098	1.0210	1.0395	1.1912	1.1070	1.1110	1.1554	1.1492
	$3d_{z^2}$	0.2322	0.2158	0.1922	0.1834	0.2336	0.2360	0.2258	0.2090
Bond M—L	4s	0.1620	0.1714	0.1690	0.2036	0.1370	0.1620	0.1748	0.1784
	$4p_z$	0.1636	0.1216	0.1006	0.0964	0.2088	0.1634	0.1402	0.1272
	Total	0.5578	0.5088	0.4618	0.4834	0.5794	0.5614	0.5408	0.5146

[a] Metal-nitrogen bond along z axis.

The Wolfsberg-Helmholz computational procedure in the SCCC modification of Ballhausen and Gray[7] was adopted. Use has been made of the orbital set 2 and the parameterization fully described in the previous paper.[4]

The VSIE of the in-plane ligand orbitals has always been assumed charge-independent. Four different values were assigned to the VSIE of the axial nitrogen orbitals in order to simulate different axial ligands, that is A) −84.4 kK (corresponding to the IP of NH_3), B) −100 kK, C) −114 kK (corresponding to the energy of 2pσ nitrogen orbital) and D) −125 kK. The σ-type MO's span the irreducible representations a_g, b_{1g}, b_{2u}, b_{3u}. The π-type MO's span a_u, b_{1u}, b_{2g}, b_{3g}. The interatomic overlap populations were evaluated by Mulliken's[8] method.

Electronic Structures. The charges on the ligand atoms and the electronic configuration of the metal atom are reported in Table I.

The effect of the increasing energy of the 2pσ(L) orbital is reflected in the increase of the positive charge on L, (*i.e.* in increasing σ donation from L through the L→M bond) and in the decrease of the charge on metal, carbon and nitrogen atoms of the chelate ring. For the same VSIE of the axial nitrogen, the variations of the charges on the ligand atoms are larger in the Co^{III} than in Fe^{II} models, while the net charges on the metal are about the same. The relative charge on the oxygen atoms does not change significantly.

The interatomic overlap populations between metal orbitals and in-plane as well as axial nitrogen orbitals are reported in Table II.

The main contributions to the equatorial σ-bonds are from the interaction of the $3d_{xy}$ and 4s metal orbitals with the 2pσ(N) orbital. The overlap population of the π-bonds is originated primarily from the $3d_{yz}$ and $4p_z$ metal orbitals and that of the M—N axial bond from the interaction of $3d_{z^2}$, 4s, $4p_z$ metal orbitals with 2pσ(L), no contribution being predominant over the others.

With increasing donor power of the axial ligand, the axial σ- and equatorial π-overlaps increase (with the exception of case D of Fe^{II} and case C of Co^{III}), while the equatorial σ-overlap slightly decreases. Assuming that the present figures may be regarded as an approximate measure of the bond strength, the total overlaps indicate a slight weakening of the equa-

(7) C. J. Ballhausen and H. B. Gray, « Molecular orbital theory », W. A. Benjamin, Inc., New York, 1964.
(8) R. S. Mulliken, *J. Chem. Phys.*, *23*, 1833, 1841, 2338, 2343 (1955).

torial and strengthening of the axial bonds.

Comparing the Fe^{II} and Co^{III} models, it can be seen from the $3d_{yz}$ contribution to the π-overlap and the strength of π-bonds that the extent of conjugation is higher in the former. On the other hand the σ-bonds are slightly stronger in the Co^{III} models.

From the trends of charges and overlap interatomic populations with increasing $2p\sigma(L)$ energy, it can be concluded that the electronic charge donated by the axial ligand does not remain only on the metal but is partly widespread over the other atoms of the chelate ring. In the present calculation scheme this is possible only through the π delocalization, as pointed out previously by Dale *et al.*[2]

Energy Diagrams. The energy levels against the energy of the axial ligand orbital $2p\sigma(L)$ (decreasing from A to D) are depicted in Figures 2 and 3. The highest level $5b_{1u}$, which is mainly $4p_z$ in character, is not reported. Energy values, atomic orbital coefficients and electronic populations of the relevant MO's are reported in Tables III and IV.

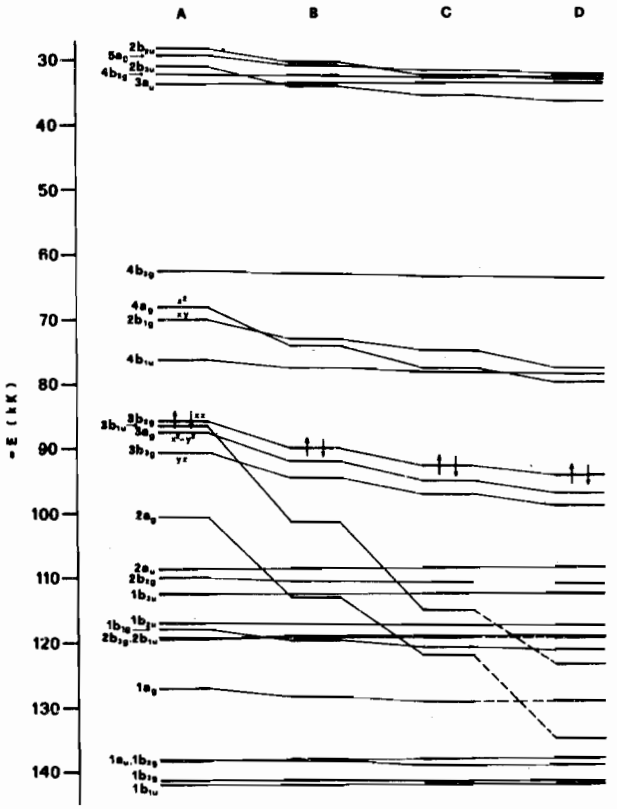

Figure 2. MO energy levels of the $Fe^{II}(Dmg)_2L_2$ complex.

Generally, the MO's which have the largest contribution of metal 3d atomic orbitals are:

$$3b_{3g} \sim 3d_{yz};\quad 3a_g \sim 3d_{x^2-y^2};\quad 3b_{2g} \sim 3d_{xz};\quad 2b_{1g} \sim 3d_{xy};\quad 4a_g \sim 3d_{z^2}$$

which shall be considered as « d » orbitals.

Since the axial ligand orbitals span the a_g and b_{1u} symmetry species, only the MO's belonging to these species and built from appreciable contribution of $2p\sigma(L)$ orbitals, *i.e.* the $3b_{1u}$, $2a_g$ and $4a_g$ MO's, undergo most important increases in energy going from D to A case. Nevertheless an overall raise of some 10 kK is observed for all MO's having some metal 3d character.

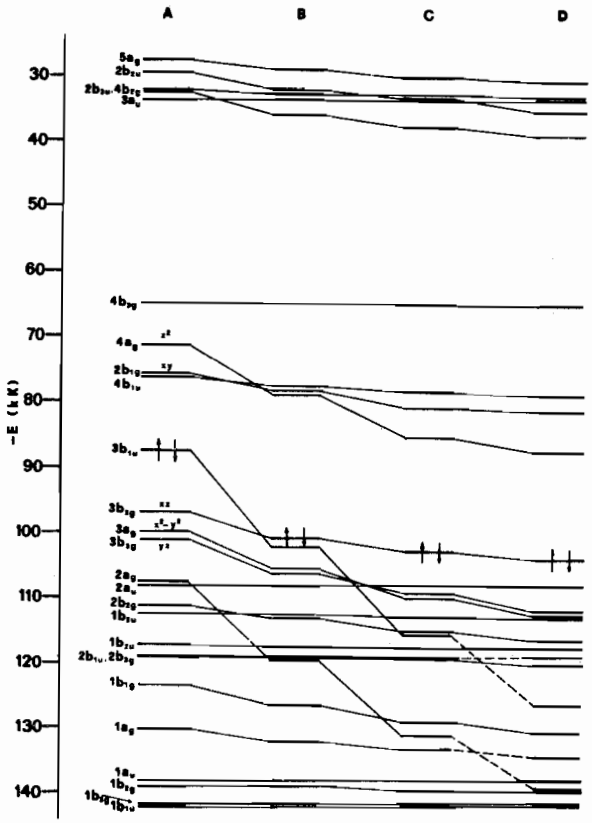

Figure 3. MO energy levels for the $Co^{III}(Dmg)_2L_2$ complex.

The different extent of changes in energy of several MO's causes inversions in the ordering of some levels. Thus the energy of the antibonding orbital $4a_g$ is higher than that of the antibonding $2b_{1g}$ in A case, but lower in the B, C, D cases for both the Fe^{II} and Co^{III} models. The lowest unfilled MO is the $4b_{1u}$ (mainly ligand in character) in the A, B, C cases for Fe^{II} and in the A case for Co^{III}, while it is the $4a_g$ in the other cases. In the case D, the MO's having the same character as the $3b_{1u}$ and $2a_g$ MO's in the cases A, B, C must be identified as the $2b_{1u}$ and $1a_g$ respectively; this fact is represented bydashed lines in the diagrams.

By increasing the σ-donor power of the axial ligand, the participation of $3d_{z^2}$ to the $4a_g$ MO decreases as does that of metal $4p_z$ to the $4b_{1u}$ MO. On the other hand,. the contribution of the $3d_{xy}$ increases in the $2b_{1g}$ MO.

In the filled frontier orbital region, there are interesting differences between Fe^{II} and Co^{III} models. In the Fe^{II} models the $3b_{2g}$, $3a_g$, $3b_{3g}$ MO's remain mainly $3d_{xz}$, $3d_{x^2-y^2}$, $3d_{yz}$ respectively, for all considered cases. The only crossing in this region is due to the insertion of $3b_{1u}$ MO (essentially $2p\sigma(L)$) between $3b_{2g}$ and $3a_g$ MO's in the case A. The last filled orbital in the Fe^{II} models remains in all cases the $3b_{3g}$ MO. On the other hand in the CO^{III} models, the $3b_{2g}$

Table III. Coefficients and populations of frontier MO's of iron complex. The first number is the orbital coefficient; the second is the electronic population. For ligand atoms coefficient is for symmetry functions; population is for all atoms. * Unfilled MO.

MO	Case	Energy (kK)	$3d_{x^2-y^2}$		$3d_{z^2}$		4s		Axial Ligand		N(2pσ)	
	A	−100.51	−0.0061	0.0000	0.5757	0.3915	0.2635	0.1069	0.6353	0.5015	−0.0198	0.0001
$2a_g$	B	−112.95	0.0112	0.0001	0.4770	0.2866	0.2320	0.0880	0.7258	0.6218	−0.0625	0.0028
	C	−124.60	0.0278	0.0010	0.4318	0.2508	0.1410	0.0340	0.7597	0.6550	−0.2396	0.0588
	D [a]	−134.90	−0.0129	0.0002	0.2629	0.0984	0.2702	0.1370	0.8035	0.7303	0.1594	0.0341
	A	−87.27	0.9918	0.9822	−0.0905	0.0083	0.0815	0.0079	0.0275	0.0009	0.0285	0.0007
$3a_g$	B	−92.05	0.9905	0.9799	−0.1062	0.0112	0.0787	0.0074	0.0251	0.0007	0.0305	0.0008
	C	−95.19	0.9895	0.9779	−0.1168	0.0136	0.0770	0.0071	0.0231	0.0005	0.0318	0.0009
	D	−97.02	0.9888	0.9764	−0.1231	0.0152	0.0762	0.0069	0.0215	0.0004	0.0325	0.0010
	A	−68.02	−0.1007	0.0086	−0.8173	0.5573	0.1635	0.0319	0.6196	0.3260	−0.3658	0.0800
$4a_g$ *	B	−73.83	−0.1066	0.0098	−0.8744	0.6499	0.0903	0.0095	0.5553	0.2419	−0.3697	0.0885
	C	−77.64	−0.1114	0.0141	−0.9072	0.7124	0.0438	0.0019	0.4972	0.1796	−0.3741	0.0950
	D	−79.83	−0.1145	0.0114	−0.9236	0.7461	0.0184	0.0001	0.4567	0.1426	−0.3778	0.0990

Mo	Case	Energy (kK)	$4p_z$		Axial Ligand		N(2pπ)		C(2pπ)		O(2pπ)	
	A	−86.53	0.2073	0.0928	0.9004	0.8515	0.1330	0.0177	−0.2083	0.0367	−0.0545	0.0022
$3b_{1u}$	B	−101.33	0.1449	0.0521	0.9534	0.9392	0.0194	0.0007	−0.0912	0.0078	−0.0050	0.0020
	C	−115.10	0.1151	0.0360	0.9596	0.9451	−0.0390	0.0009	−0.1104	0.0132	0.0734	0.0030
	D [b]	−126.09	0.1121	0.0360	0.9667	0.9583	0.0086	0.0003	0.0025	0.0004	−0.0697	0.0047
	A	−76.34	−0.3090	0.1337	0.3772	0.1167	−0.6326	0.3104	0.7267	0.3998	0.2378	0.0394
$4b_{1u}$*	B	−77.59	−0.3561	0.1828	0.2219	0.0319	−0.6323	0.3155	0.7493	0.4290	0.2404	0.0405
	C	−78.13	−0.3705	0.1983	0.1787	0.0174	−0.6255	0.3105	0.7514	0.4334	0.2389	0.0402
	D	−78.40	−0.3768	0.2050	0.1607	0.0125	−0.6215	0.3073	0.7520	0.4350	0.2380	0.0399

		Energy (kK)	3d		N(2pσ)		N(2pπ)		C(2pπ)		O(2pπ)	
	A	−70.17	−0.9199 [c]	0.7350 [c]	0.6132	0.2650						
$2b_{1g}$*	B	−73.03	−0.8960	0.6873	0.6544	0.3127						
	C	−74.78	−0.8784	0.6536	0.6814	0.3463						
	D	−75.74	−0.8675	0.6335	0.6969	0.3665						
	A	−109.99	−0.2200 [d]	0.0603 [d]			−0.6142	0.3885	−0.3290	0.1594	0.6750	0.3917
$2b_{2g}$	B	−110.41	−0.2787	0.0925			−0.5993	0.3713	−0.3157	0.1475	0.6712	0.3887
	C	−110.80	−0.3294	0.1255			−0.5842	0.3540	−0.3030	0.1364	0.6661	0.3839
	D	−111.09	−0.3643	0.1511			−0.5724	0.3407	−0.2936	0.1285	0.6616	0.3796
	A	−85.81	0.9616 [d]	0.9119 [d]			−0.1493	0.0174	−0.2338	0.0639	0.0966	0.0067
$3b_{2g}$	B	−90.04	0.9473	0.8808			−0.1979	0.0327	−0.2462	0.0735	0.1324	0.0130
	C	−92.71	0.9313	0.8477			−0.2371	0.0486	−0.2590	0.0833	0.1641	0.0200
	D	−94.20	0.9183	0.8218			−0.2632	0.0610	−0.2683	0.0906	0.1863	0.0265
	A	−90.64	0.8732 [e]	0.7847 [e]			0.2357	0.0454	−0.4367	0.1625	−0.0943	0.0070
$3b_{3g}$	B	−94.58	0.8955	0.8190			0.1771	0.0260	−0.4134	0.1507	−0.0725	0.0040
	C	−97.23	0.9050	0.8328			0.1411	0.0164	−0.4049	0.1482	−0.0548	0.0020
	D	−98.79	0.9088	0.8377			0.1206	0.0119	−0.4027	0.1488	−0.0435	0.0015
	A	−62.48	0.4877 [e]	0.1952 [e]			−0.8081	0.4190	0.7055	0.3402	0.2661	0.0456
$4b_{3g}$*	B	−63.11	0.4384	0.1531			−0.8228	0.4378	0.7252	0.3611	0.2723	0.0480
	C	−63.44	0.4110	0.1320			−0.8298	0.4471	0.7351	0.3718	0.2753	0.0491
	D	−63.60	0.3966	0.1215			−0.8331	0.4517	0.7399	0.3771	0.2767	0.0497

[a] $1a_g$ (see text); [b] $2b_{1u}$ (see text); [c] $3d_{xy}$; [d] $3d_{xz}$; [e] $3d_{yz}$.

and $2b_{2g}$ MO's are formed by more extended « mixing » of metal 3d and chelating ring orbitals. The $3b_{2g}$ MO becomes progressively less metal in character going from A to D cases, while the reverse is true for the $2b_{2g}$ MO, so that this latter must be regarded as « $3d_{xz}$ » MO in the C and D cases. The $3b_{3g}$ and $3a_g$ MO's remain mainly 3d in character. The $3b_{1u}$ MO crosses the MO pattern and becomes the highest filled MO in the A case. The last filled MO in Co^{III} models is thus represented by $3b_{1u}$ (A) or $3b_{3g}$ MO's (B, C, D).

The existence of the close lying antibonding «$3d_{z^2}$» and «$3d_{xy}$» orbitals separated from the bonding «$3d_{xz}$», «$3d_{yz}$» and «$3d_{x^2-y^2}$» orbitals reproduces the 3d orbital pattern in a weakly distorted tetragonal field. The energy separation is greater (~ 10 kK) in Co^{III} than in Fe^{II} models.

The relative position and energy difference of «$3d_{z^2}$» and «$3d_{xy}$» MO's depend on the energy difference between axial 2pσ(L) and equatorial 2pσ(N) orbitals. The inversion is thus due to the fact that this difference is >0 for A models and <0 for B, C, D models. As a consequence the energy gap between the last filled and the first empty MO's increases from D to B but strongly decreases form B to A in the Co^{III} cases. On the contrary it continuously decreases in Fe^{II} models.

Electronic Spectra. Even though one-electron transitions obtained from the present calculation are not expected to reproduce the observed spectra, some general comments can however be made.

Table IV. Coefficients and populations of frontier MO's of cobalt complex. The first number is the orbital coefficient; the second is the electronic population. For ligand atoms coefficient is for symmetry functions; population is for all atoms. * Unfilled MO.

MO	Case	Energy (kK)	$3d_{x^2-y^2}$		$3d_{z^2}$		4s		Axial Ligand		N(2pσ)	
	A	−108.36	−0.0407	0.0018	0.6854	0.5222	0.2421	0.1140	0.5136	0.3554	0.0753	0.0066
$2a_g$	B	−119.77	−0.0206	0.0005	0.5806	0.3918	0.2713	0.1196	0.6182	0.4816	0.0682	0.0062
	C	−130.76	−0.0217	0.0006	0.4608	0.2593	0.2849	0.1390	0.6948	0.5829	0.1153	0.0180
	D [a]	−139.84	0.0010	0.0000	0.4505	0.2591	0.2243	0.0890	0.7456	0.6514	−0.0078	0.0000
	A	−99.93	0.9901	0.9781	−0.0509	0.0025	0.1014	0.0133	0.0506	0.0053	0.0532	0.0072
$3a_g$	B	−105.65	0.9885	0.9749	−0.0880	0.0076	0.0963	0.0120	0.0450	0.0024	0.0551	0.0036
	C	−109.83	0.9864	0.9796	−0.1122	0.0126	0.0939	0.0115	0.0412	0.0018	0.0569	0.0034
	D	−112.50	0.9848	0.9674	−0.1270	0.0162	0.0929	0.0113	0.0387	0.0015	0.0583	0.0036
	A	−71.73	−0.0866	0.0060	−0.7091	0.3852	0.1907	0.0427	0.7120	0.4555	−0.4146	0.1100
$4a_g$*	B	−79.05	−0.0934	0.0071	−0.7782	0.4816	0.1027	0.0124	0.6636	0.3709	−0.4270	0.1279
	C	−84.35	−0.0996	0.0081	−0.8233	0.5529	0.0387	0.0015	0.6087	0.2930	−0.4402	0.1445
	D	−87.62	−0.1039	0.0088	−0.8471	0.5941	−0.0009	0.0001	0.5653	0.2400	−0.4504	0.1570

MO	Case	Energy (kK)	$4p_z$		Axial Ligand		N(2pπ)		C(2pπ)		O(2pπ)	
	A	−87.33	−0.2439	0.1234	−0.8663	0.8026	−0.1498	0.0225	0.2422	0.0485	0.0616	0.0028
$3b_{1u}$	B	−101.96	−0.1760	0.0728	−0.9344	0.9136	−0.0220	0.0010	0.1151	0.0125	0.0047	0.0000
	C	−115.63	−0.1378	0.0482	−0.9374	0.9106	0.0597	0.0026	0.1566	0.0268	0.1143	0.0117
	D [b]	−119.08	−0.1393	0.0525	−0.9519	0.9387	−0.0086	0.0003	0.0001	0.0268	0.0922	0.0084
	A	−76.35	−0.2977	0.1720	0.4310	0.1540	−0.6244	0.3005	0.7175	0.3897	0.2348	0.0384
$4b_{1u}$*	B	−77.90	−0.3563	0.1760	0.2640	0.0465	−0.6263	0.3087	0.7478	0.4285	0.2387	0.0400
	C	−78.63	−0.3757	0.1960	0.2147	0.0262	−0.6175	0.3023	0.7515	0.4353	0.2369	0.0396
	D	−79.02	−0.3844	0.2056	0.1938	0.0191	−0.6120	0.2979	0.7526	0.4379	0.2356	0.0393

MO			3d		N(2pσ)		N(2pπ)		C(2pπ)		O(2pπ)	
	A	−76.30	−0.8497 [c]	0.5969 [c]	0.7267	0.4031						
$2b_{1g}$	B	−78.82	−0.8124	0.5332	0.7704	0.4668						
	C	−80.43	−0.7839	0.4875	0.7996	0.5125						
	D	−81.35	−0.7655	0.4593	0.8169	0.5407						
	A	−111.25	−0.4124 [d]	0.1883 [d]			−0.5581	0.3240	−0.2844	0.1208	0.6500	0.3668
$2b_{2g}$	B	−112.89	−0.5811	0.3597			−0.4771	0.2400	−0.2275	0.0788	0.6045	0.3215
	C	−114.83	0.7094	0.5250			0.3866	0.1601	0.1698	0.0449	−0.5497	0.2699
	D	−116.43	0.7757	0.6215			0.3229	0.1131	0.1320	0.0276	−0.5124	0.2376
	A	−97.11	0.9003 [d]	0.7812 [d]			−0.2975	0.0804	−0.2686	0.0919	0.2217	0.0383
$3b_{2g}$	B	−101.04	0.8005	0.6140			−0.4131	0.1618	−0.3145	0.1328	0.3362	0.0900
	C	−103.15	0.6870	0.4447			−0.4974	0.2394	−0.3479	0.1660	0.4283	0.1497
	D	−104.13	0.6082	0.3437			−0.5400	0.2849	−0.3635	0.1829	0.4786	0.1883
	A	−101.15	0.9270 [e]	0.8666 [e]			0.0817	0.0050	−0.3689	0.1277	−0.0219	0.0004
$3b_{3g}$	B	−106.11	0.9212	0.8500			0.0166	0.0020	−0.3889	0.1491	0.0324	0.0008
	C	−109.59	0.8975	0.8019			−0.0418	0.0030	−0.4275	0.1868	0.1015	0.0087
	D	−111.64	0.8630	0.7373			−0.0879	0.0099	−0.4667	0.2276	0.1701	0.0250
	A	−64.84	0.3435 [e]	0.0901 [e]			−0.8365	0.4597	0.7575	0.3988	0.2806	0.0514
$4b_{3g}$*	B	−65.15	0.3107	0.0711			−0.8419	0.4676	0.7662	0.4286	0.2839	0.0401
	C	−65.32	0.2911	0.0608			−0.8447	0.4718	0.7709	0.4144	0.2844	0.0530
	D	−65.41	0.2802	0.0554			−0.8460	0.4740	0.7733	0.4173	0.2851	0.0533

[a] $1a_g$ (see text); [b] $2b_{1u}$ (see text); [c] $3d_{xy}$; [d] $3d_{xz}$; [e] $3d_{yz}$.

Table V summarizes the symmetry-allowed one-electron transitions up to 60 kK with comparatively large oscillator strength.

The experimental spectra of the present type of complexes show intense absorptions as poorly resolved envelops of relatively close lying bands starting from ~15 kK in Fe^{II} and from ~20 kK in Co^{III} derivatives.[9,10,11,12]

In the $Fe^{II}(Dmg)_2L_2$ complexes with nitrogen in the axial position, a prominent band is observed at about 19 kK moving to shorter frequency as the σ-donor strength of L increases. It was assigned to an electron transfer from one d_ϵ orbital to a higher electron state of iron, possibly 4p, strongly interacting with the ligand, so that the electron is partially transferred to the ligand.[11] From the present calculation, the $3b_{3g} \rightarrow 4b_{1u}$ transition, CT from metal to ligand in character, falls in the same range of frequency and shows the same trend as the observed band with the increasing σ-donor power of L.

Two strong bands recorded at 26-30 and ~33 kK in the spectra of $Co^{III}(Dmg)_2L_2$ complexes with L= substituted anilines were investigated by Matsumoto *et al.*[12] The first band shifts to shorter frequency with increasing basicity of L and was assigned to

(9) A. V. Ablov and M. P. Filippov, *J. Inorg. Chem.* USSR, 3, 1565 (1958); *Russian J. Inorg. Chem.*, *4*, 1004 (1959).
(10) I. Csaszar and K. Fügedi, *Acta Chim. Hung.*, *32*, 451 (1962).
(11) B. A. Jillot and R. J. P. Williams, *J. Chem. Soc.*, *1958*, 462.
(12) C. Matsumoto, T. Kato and K. Shirira, *Nippon Kagaku Zasshi*, *86*, 1266 (1965).

Table V. Electronic transitions

Complex	Iron								Cobalt							
Case	A		B		C		D		A		B		C		D	
Transition	E[a]	f														
$3b_{3g} \rightarrow 4b_{1u}$	14.3	0.14	17.0	0.14	19.1	0.13	20.3	0.13	24.8	0.11	28.2	0.12	30.9	0.13	32.6	0.14
$3b_{1u} \rightarrow 4a_g$	18.5	0.24	27.5	0.32	37.4	0.35	46.2[b]	0.37[b]	15.6	0.25	22.9	0.36	31.2	0.42	39.0[b]	0.47[b]
$3b_{1u} \rightarrow 4b_{3g}$	24.0	0.06	38.2	0.01	51.0	0.01	55.4[c]	0.02[c]	22.5	0.09	36.8	0.02	50.3	0.01	53.6[c]	0.02[c]
$2a_g \rightarrow 4b_{1u}$	24.1	0.06	35.6	0.04	46.5	0.03	50.4	0.00	32.0	0.06	41.9	0.05	52.1	0.04	55.2	0.00
$2b_{2g} \rightarrow 4b_{1u}$	33.6	0.18	32.8	0.17	32.7	0.16	32.6	0.16	34.9	0.16	35.0	0.14	36.2	0.11	37.4	0.09
$1b_{3u} \rightarrow 2b_{1g}$	42.4	0.40	39.3	0.43	37.7	0.44	36.8	0.45	36.1	0.48	33.8	0.50	32.4	0.51	31.5	0.52
$2b_{3g} \rightarrow 4b_{1u}$	42.5	0.04	41.3	0.04	40.9	0.04	40.7	0.04	42.7	0.03	41.4	0.03	41.1	0.02	41.0	0.01
$1b_{3u} \rightarrow 4a_g$	44.2	0.04	38.5	0.08	34.8	0.07	32.7	0.07	40.6	0.10	33.6	0.09	28.4	0.08	25.3	0.07
$1b_{2u} \rightarrow 2b_{1g}$	46.8	0.28	44.1	0.29	42.5	0.31	41.6	0.32	40.8	0.34	38.6	0.35	37.1	0.36	36.4	0.37
$2a_u \rightarrow 4b_{3g}$	46.0	0.41	45.3	0.41	45.0	0.42	44.8	0.42	43.6	0.41	43.3	0.42	43.1	0.42	43.0	0.42
$1b_{2u} \rightarrow 4a_g$	48.9	0.14	43.3	0.13	39.6	0.12	37.5	0.11	45.4	0.17	38.4	0.15	33.3	0.14	30.1	0.13

[a] Energy in Kilokaysers. [b] $2b_{1u} \rightarrow 4a_g$ (see text). [c] $2b_{1u} \rightarrow 4b_{3g}$ (see text).

a CT from the axial ligand to the metal. The second band is very little affected by changing the axial ligand. In the present calculation, both the transitions $3b_{3g} \rightarrow 4b_{1u}$ and $3b_{1u} \rightarrow 4a_g$ exhibit the same behaviour and are very sensitive to the axial ligand. They could be related to the first experimental band. On the other side, the transitions $2b_{2g} \rightarrow 4b_{1u}$ and $1b_{3u} \rightarrow 2b_{1g}$ in the range 31-42kK are relatively less dependent on the axial ligand and CT in nature, in particular the second one involves CT from equatorial ligand to a « 3d » orbital The band observed at ~33 kK may be assigned to these transitions.

The $2a_u \rightarrow 4b_{3g}$ transition represents a $\pi \rightarrow \pi^*$ transition of the dimethylglyoxime moiety almost insensitive to the nature of L. It is calculated at 45 and 42 kK in Fe^{II} and Co^{III} models, in good agreement with the absorptions observed at 44 and 40.5 kK in $Fe^{II}(Dmg)_2(NH_3)_2$ and $Co^{III}(Dmg)_2(NH_3)_2$ respectively.[10]

The symmetry-forbidden d–d bands, which are predicted in the 15-25 (Fe^{II}) and 20-30 kK (Co^{III}) regions, are probably obscured by the more intense bands due to the symmetry-allowed transitions.

Co^{II} Models and g Factors. For the complexes of the type $Co^{II}(Dmg)_2L_2$ the results of the calculation show that the ordering and character of the MO's are almost the same as in Co^{III} derivatives. Thus, the unpaired electron is virtually located in the first unfilled orbital which happens to be the $4a_g$ MO in the B, C, D cases of the Co^{III} as illustrated by the energy diagrams reported in Figure 3. In the case A it is assigned to the $2b_{1g}$ MO instead of $4b_{1u}$ MO, owing to an inversion of these two very close levels.

The following estimates of the components of the spectroscopic g factor:

case	A	B	C	D
$g_{\parallel}$	2.044	2.000	2.000	2.000
$g_{\perp}$	2.008	2.028	2.035	2.040

were obtained on the basis of the Abragam and Pryce method[13] as developed by Maki and McGarvey,[14] assuming for Co^{II} the ^4F ground state and a spin-orbit coupling constant of -180 cm^{-1}.

(13) A. Abragam and M. H. L. Pryce, *Proc. Roy. Soc., A205,* 135 (1951).
(14) A. H. Maki and B. R. McGarvey, *J. Chem. Phys., 29,* 31 (1958).

The $g_{\perp}$ are mean values of g_{xx} and g_{yy} which are not equal in the assumed rhombic geometry. The estimates are low in comparison with a mean value of 2.2 generally found for Co^{II} complexes.[15,16] This may perhaps be ascribed to the fact that in the assumed model the 2s nitrogen orbitals are not taken into account.

Both the energy patterns and g factors calculated for certain range of energy of $2p\sigma$ orbital of the axial ligand (cases B, C, D) indicate that the unpaired electron has to be located in the « $3d_{z^2}$ » MO, in agreement with the assignment proposed for similar compounds on the basis of ESR spectra analysis.[15,16] In the case A the unpaired electron is predicted to be situated in the « $3d_{xy}$ » MO.

Mössbauer Spectrum. The electronic structure calculated for the Fe^{II} complex allows to obtain some informations about the most important parameters of ^{57}Fe Mössbauer spectra. The following estimates for quadrupole splitting have been obtained by the approximate treatment described in the previous paper:[4]

Model	A	B	C	D
Δ (cm/sec)	0.150	0.162	0.184	0.198

In agreement with the spectral data on structural similar $Fe^{II}(niox)_2L_2$ complexes[2] the evaluated quadrupole splitting turns out to increase moderately as the σ-donor strength of the axial ligands is lowered. The order of magnitude of the calculated quadrupole splitting appears well compatible with that experimentally found by Ablov *et al.*[17] on $Fe(Dmg)_2Py_2$, (0.18 cm/sec.). However it should be noted that in the latter complex the axial ligand displays σ-donor as well as π-acceptor properties.

The isomeric shift is a measure of the total s density at the iron nucleus, in such a way that increasing negative values of isomeric shift correspond to increased values of s density. As can be seen from Table II, 4s density raises as the σ-donor power of the axial ligands increases. This tendency might suggest that the corresponding Mössbauer spectra should exhibit

(15) G. N. Schrauzer and L. P. Lee, *J. Am. Chem. Soc., 90,* 6541 (1968).
(16) J. M. Assour, *J. Am.Chem. Soc., 87,* 4701 (1965).
(17) A. V. Ablov, V. I. Gol'danskii, R. A. Stukan and E. F. Makarov, *Dokl. Akad. Nauk SSSR, 170,* 128 (1966).

an increasing negative shift. This behaviour would be analogous to that found experimentally on $Fe^{II}(niox)_2L_2$.[2]

As concerns the $\partial^2V/\partial z^2$ parameter, the calculations yield a positive sign for the models B, C and D, but a negative sign for the A model. Lack of spectral data does not permit to confirm the above signs in the present compounds. However the first situation turns out to be in agreement with the experimental data obtained by Dale *et al.*[18] leading to the conclusion that the sign of $\partial^2V/\partial z^2$ is positive.

Finally, the assumption that $Co^{III}(Dmg)_2(NH_3)_2$ does not undergo fragmentation during the radioactive decay of ^{57}Co, allows to gather some information about the quadrupole splitting and isomeric shift on the basis of the evaluated electronic structure. The assumed parameters for ^{57}Co are as follows: the nuclear quadrupole moment of 0.404 barns[19] relative to ^{59}Co, the mean value $<r^{-3}>$ of 5.2[21] a.u. and the Sternheimer antishielding factors already adopted for ^{57}Fe. The following estimates of quadrupole splitting have been obtained:

Model	A	B	C	D
Δ (cm/sec)	0.171	0.237	0.349	0.419

The behaviour of quadrupole splitting and isomeric shift against the σ-donor of the axial ligand is quite similar but more pronounced than in Fe^{II} case, *i.e.* they decrease as the σ-donor power of axial ligand increases.

Recently published results[21] obtained on some analogues of Vitamine B_{12} and Co^{II}phtalocyanine complexes with a series of essentially σ-donor axial ligands show that the quadrupole splitting and the isomeric shift decrease when the σ-donor power increases. These results are in agreement with those expected from calculations for the $^{57}Co(Dmg)_2L_2$ complexes.

However there is some doubt if these compounds do not undergo fragmentation because they have not a large conjugated ring which could prevent the multicentre coulombic repulsions which are largely respinsible of fragmentation. Indeed evidence for degradation has been found on $^{57}Co^{II}$bis-acetylacetone.[21]

Acknowledgment. This work has been in part supported by the Consiglio Nazionale delle Ricerche of Italy.

(18) B. W. Dale, R. J. P. Williams, P. R. Edwards and C. E. Johnson, *Trans. Far. Soc.*, *64*, 3011 (1968).
(19) B. A. Scott and R. A. Bernsheim, *J. Chem. Phys.*, *44*, 2004 (1966).
(20) A. Abragam, J. Horowitz and M. H. L. Pryce, *Proc. Roy. Soc.*, *A 230*, 169 (1955).
(21) A. Nath,M. Harpold, M. P. Klein and W. Kündig, *Chem. Phys. Lett.*, *2*, 471 (1968).